

Biomorphic SiC-ceramic prepared by Si-vapor phase infiltration of wood

E. Vogli, H. Sieber, P. Greil*

Department of Materials Science Glass and Ceramics, University of Erlangen-Nuremberg, D-91058 Erlangen, Germany

Received 8 October 2001; received in revised form 18 January 2002; accepted 6 March 2002

Abstract

The conversion of bioorganic structures like wood or ligninocellulosic fibers into porous microcellular SiC-ceramics is a novel manufacturing technology. Coniferous wood (pine) was transformed by high-temperature pyrolysis into carbon preforms and subsequently converted into biomorphic SiC-ceramics by Si-vapor infiltration under inert atmosphere. The morphology of the initial wood structure is retained. The infiltration of the Si-vapor phase into the C_B-template and the kinetics of the SiC-formation were investigated. The amount of residual carbon was determined by means of mass balance calculation. The macroscopical properties of the final SiC-ceramics were characterized by porosity and mechanical property measurements. © 2002 Elsevier Science Ltd. All rights reserved.

Keywords: Biotemplating; Mechanical properties; Porous ceramics; SiC; Si-vapor infiltration; Wood

1. Introduction

The fact that trees are capable of standing up as cantilever beams for hundreds of years is due to the high level of its mechanical properties.¹ The reason for this is not to be sought in one particular property, but rather in a remarkable combination of mechanical properties and in the way in which these are related to the morphology and the structure of the material. Since the first work of Thompson,² who studied the relationship between growth and shape of wood, bioorganic materials have been of considerable interest in a variety of research fields, primarily in materials science and engineering.

The microstructural morphology of wood is characterized by a cellular anisotropy and makes it an interesting raw material for structural ceramics with tailored physical and mechanical properties. Cellular SiC-ceramics manufactured by conversion of wood with different infiltration reactions yield porous materials

with an unidirectional pore structure on the micrometer level and a designed strut morphology.³

Research in ceramic engineering was concentrated on the microstructural conversion of biological fiber materials as well as of wood tissue. For example, Al₂O₃ and TiO₂ fibers were produced through sol/gel infiltration in jute fibers.^{4,5} The sol/gel infiltration method was used also to transform pyrolysed wood into porous TiO₂-ceramic by Ota et al.⁶ or to manufacture biomorphous oxide ceramics of Al₂O₃, mullite and ZrO₂ by Sieber et al.⁷ Vogt et al.⁸ infiltrated SiO₂-sol/gel to transform charcoal into SiC. Zollfrank et al.⁹ infiltrated PMPVS (polymethylphenylvinylsilsesquioxane) and PMHS (polymethylhydrosiloxane) into charcoal to produce porous SiOC-ceramics. Ota et al.¹⁰ infiltrated TEOS (tetraethylorthosilicate) into pyrolysed wood. Biomorphous porous SiC can also be manufactured by SiO-vapor¹¹ or CH₃SiCl₃-infiltration/reaction¹² into pyrolysed wood. Greil et al.,¹³ following by Shin et al.¹⁴ and Martinez-Fernandez et al.¹⁵ prepared more dense SiSiC-ceramic by Si-melt infiltration into pyrolysed wood.

In this work, the vapor phase reaction of pyrolysed pine-wood with Si-vapor and the conversion into highly porous SiC-ceramics was investigated. During conversion, the morphology of the initial wood, the wood char

* Corresponding author. Tel.: +49-9131-852-7543; fax: +49-9131-852-8311.

E-mail addresses: vogli@ww.uni-erlangen.de (E. Vogli), greil@ww.uni-erlangen.de (P. Greil).

and the final biomorphic SiC-ceramic were characterized. The carbide formation reaction and the growth behavior of the SiC during the vapour_{Si}–solid_{carbon} reaction process at 1600 °C were studied by X-ray diffraction (XRD) and scanning electron microscopy (SEM)/EDX. The mechanical behavior of ceramics derived wood was determined by ball-on-ring test.

2. Processing of biomorphic SiC ceramics

2.1. Pyrolysis of pine-wood

Pine-wood was used as the biological template structure. Pine (*Pinus sylvestris* L.) is a coniferous wood and exhibits a nearly monomodal pore distribution with a mean pore diameter of about 20 µm. It shows a uniform morphology of 90–95% tracheids, which serve for the axial water conduction and mechanical support in the living tree. The tracheids are usually about 1–5 mm long, depending on the tree species, the radial distance from the stem center, the position in the growth increment and the height in the tree. Tracheid cell walls are pierced by a large number of pits.

Carbon preforms were prepared by pyrolysing the dried (70 °C, 24 h) pine-wood in inert atmosphere. During pyrolysis, H₂O, CO and CO₂-volatiles were released. To get a crack-free carbon template a slow heating rate of 1 K/min was applied up to 500 °C.¹⁶ A higher heating rate of 5 K/min was applied up to 800 °C, where the rearrangement of the polyaromatic carbon structures takes place. The specimens were held at peak temperature for 4 h. During pyrolysis a sharp weight loss started at 220 °C and ended at about 400 °C, followed by a reduced weight loss rate. After 800 °C the final weight

loss accounts to 68% for the pine-wood. Anisotropic shrinkage in three directions (axial, tangential and radial) was associated with the pyrolysis process (Fig. 1). Despite the large weight loss during pyrolysis, the carbon template reflects the microstructure and morphology of the native specimen (Fig. 2).

2.2. Si-vapor phase infiltration

After pyrolysis, the carbon templates were reacted with Si-vapor in a glassy-carbon crucible inside an alumina tube. The Si-vapor was generated by melting of Si-powder at a temperature of 1600 °C for 1–8 h in Ar-atmosphere. The Si-vapor penetrates the pyrolysed wood templates, which were positioned in axial direction over the Si-melt (Fig. 3) and reacts with the carbon to β-SiC:



The weight gain of the samples was measured at different times during the Si-vapor infiltration. The content of SiC and unreacted C were determined from mass-balance and shrinkage measurements.

$$m_{\text{sample}} = m_{\text{SiC}} + m_{\text{C}} = V_{\text{SiC}}\rho_{\text{SiC}} + V_{\text{C}}\rho_{\text{C}} \quad (2)$$

shrinkage:

$$\Delta V = V_{\text{sample}} - V_{\text{C}}^0 + (V_{\text{P}} - V_{\text{P}}^0) \quad (3)$$

where m_{SiC} , V_{SiC} , ρ_{SiC} and m_{C} , V_{C} , ρ_{C} are the mass, volume and density of SiC and C, respectively, V_{C}^0 —the initial sample volume, V_{sample} and m_{sample} —the sample volume and mass after infiltration, V_{P}^0 and V_{P} —the

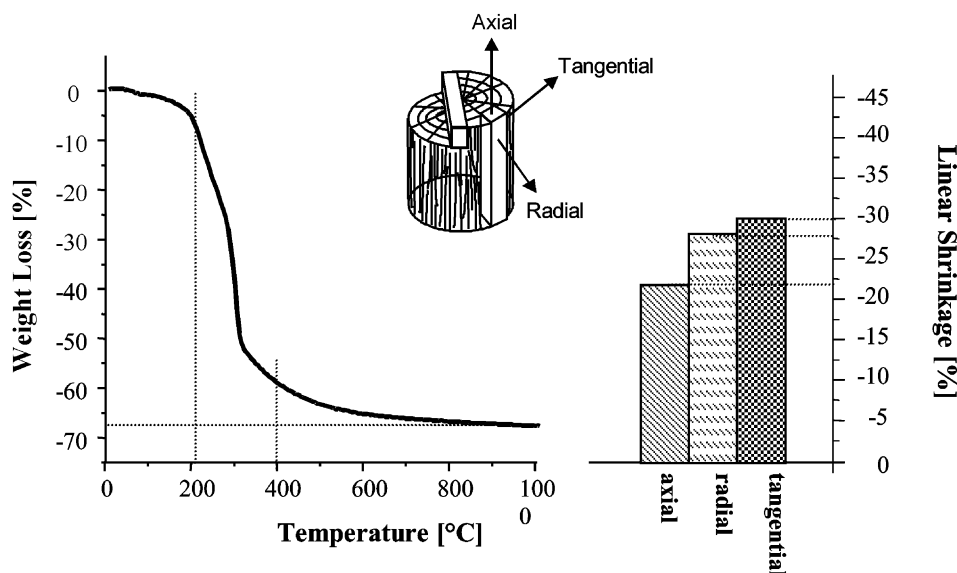


Fig. 1. Weight loss and linear shrinkage during pyrolysis (average values derived from 20 to 40 specimens).

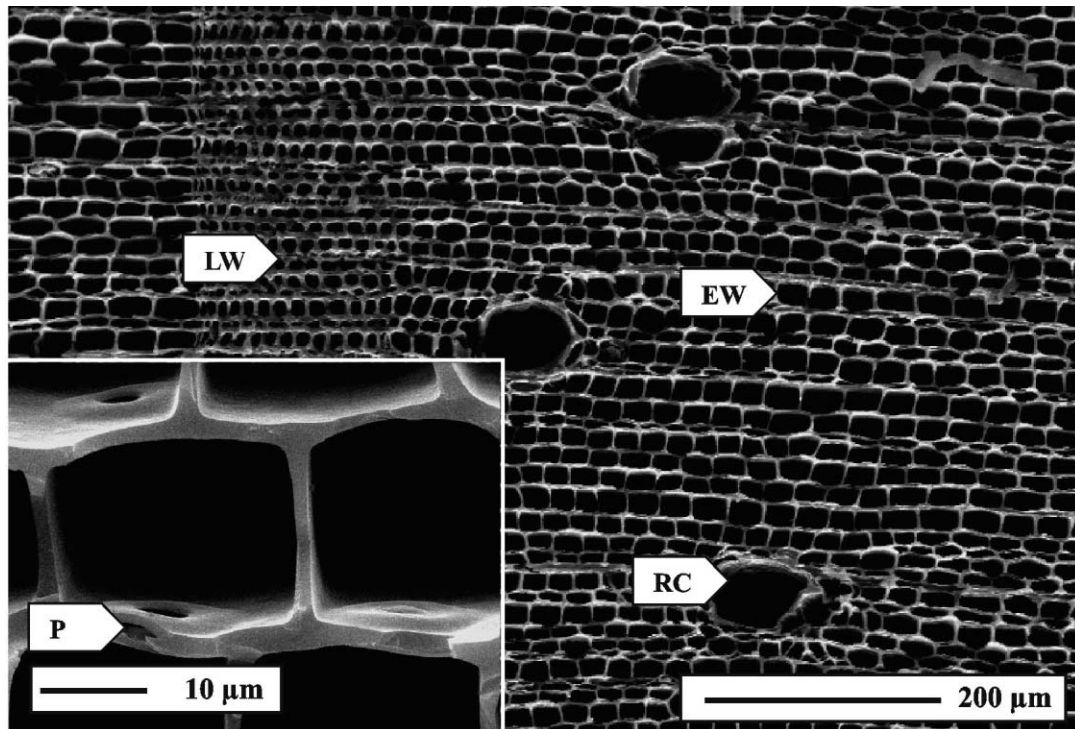


Fig. 2. Micrographs of pyrolysed Pine; (EW—Earlywood; LW—Latewood; RC—Resin canal; P—Pit).

Processing

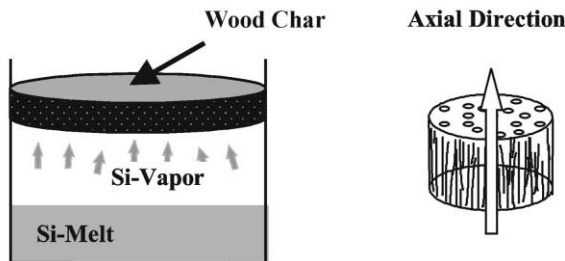


Fig. 3. Experimental set up for the Si-vapor infiltration.

initial pore volume (76% of the initial volume) and after infiltration (e.g. 71% of sample volume infiltrated for 4 h). During infiltration a linear change in porosity was assumed. An expression for the amounts of SiC and C were determined from the combining of the Eqs. 2 and 3:

$$m_{\text{SiC}} = \frac{m_{\text{sample}} - [\Delta V + V_{\text{C}}^{\circ} - (V_{\text{P}} - V_{\text{P}}^{\circ})] \rho_{\text{C}}}{\rho_{\text{SiC}} - \rho_{\text{C}}} \rho_{\text{SiC}} \quad (4)$$

$$m_{\text{C}} = m_{\text{sample}} - m_{\text{SiC}} \quad (5)$$

The manufactured SiC-specimens (cylindrical specimens with a diameter approximately 20 mm and a thickness of 2.5 mm) were mechanically tested by the ball-on-ring test using an Instron universal testing machine (4204, Instron, High Wycombe, Buckinghamshire/UK). A disc specimen is placed on a ring and

centrally loaded with a ball. The test scheme is shown in Fig. 6(a). A biaxial tensile stress-state is generated at the center of the specimen. The maximum stress components at fracture ($\sigma_{\text{max,tan}}, \sigma_{\text{max,rad}}$) were calculated from:

$$\begin{aligned} \sigma_{\text{max,tan}} &= \sigma_{\text{max,rad}} = \sigma_{\text{max}} \\ &= \frac{3P(1+\nu)}{4\pi t^2} \\ &\times \left[1 + 2\ln \frac{a}{b} + \frac{1-\nu}{1+\nu} \left\{ 1 - \frac{b^2}{2a^2} \right\} \frac{a_2}{R^2} \right] \end{aligned} \quad (6)$$

where P is maximal load, t —sample thickness, a —radius of support ring, b —radius of uniform loading region at the center (determined as $\approx t/3$), R —sample radius, and ν —Poisson's ratio ($\nu=0.25$ for SiC). The fractured surfaces were analyzed by SEM measurements (Stereoscan S 250 MK3, Cambridge Instruments, Cambridge/UK).

3. Results and discussion

The morphological properties of the pine-wood, pine-char and pine derived β -SiC are shown in Table 1. According to the reaction (1) and Table 1 the formed β -SiC exhibits a higher density, a decreased porosity and lower specific surface area compared to the C_{B} -tem-

Table 1
The properties of natural Pine, Pine-char and SiC

Pine	Wood	Char	SiC
Density (g/cm ³)			
Geometrical	0.47	0.34	1.0
Skeleton	1.4	1.4	3.1
Porosity (%)	67	76	71
Specific surface (m ³ /g)	–	46	3.3

Fig. 4(a) shows the calculated mass change [Eqs. (4) and (5)] after infiltration at 1600 °C for different times. After 4 h of Si-vapor infiltration at 1600 °C the specimens exhibits a SiC-content of 92%, after 8 h infiltration-time, the SiC-content increased only to 94%.

XRD investigation [Fig. 4(b)] shows β -SiC as the ceramic product phase. The (111) peak of β -SiC increased with time, whereas the (0002) peak of carbonized wood

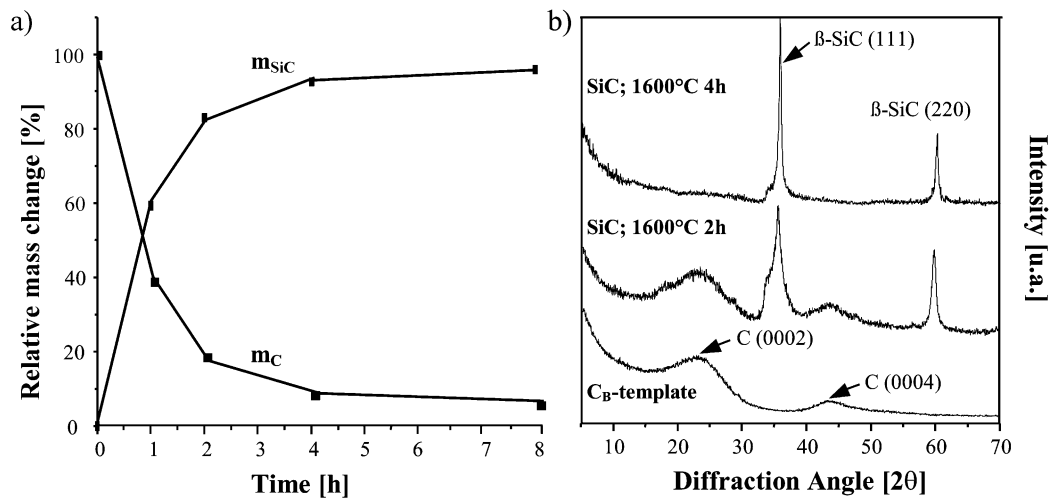


Fig. 4. (a) Weight increase at 1600 °C for different infiltration/reaction times. (b) XRD-analysis.

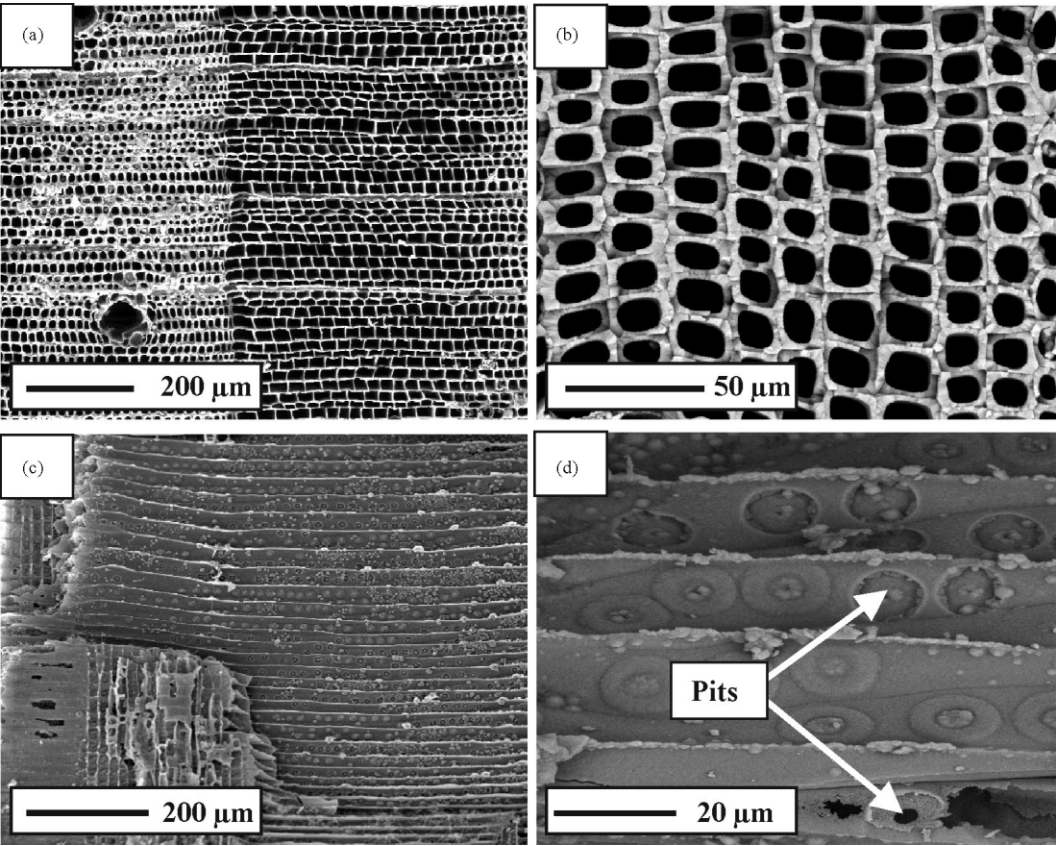


Fig. 5. Porous β -SiC ceramic manufactured by Si-vapor infiltration of pyrolysed pine-wood at 1600 °C for 4 h: SiC derived from pine in axial (a)–(b) and tangential direction (c)–(d).

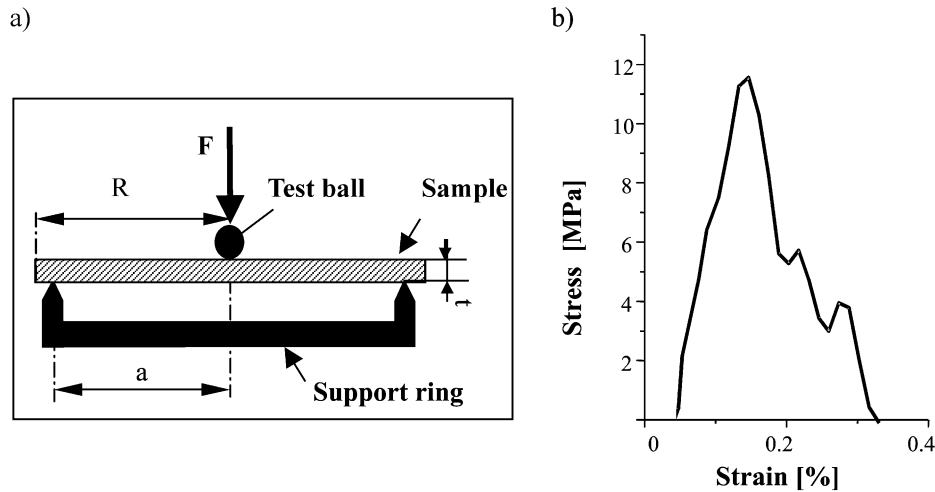


Fig. 6. (a) Ball-on-ring test schema. (b) Stress–strain behavior.

decreased. During infiltration, no Si-peaks could be detected in the specimens. In the sample infiltrated at 1600 °C for 4 h only the sharp β -SiC peaks could be observed. Fig. 5 shows the cellular microstructure of the SiC-ceramic. After the Si-vapor infiltration and reaction process, the SiC material reproduces the cellular morphology of natural wood. It exhibits a relatively homogeneous strut thickness of about 2 μm . The specific surface area was 46 m^2/g in the carbon template, which was reduced to 3.3 m^2/g in the biomorphic SiC. The density increased from 0.34 to 1 g/cm^3 .

The biaxial bending strength of the biomorphic SiC-ceramics was determined by a ball-on-ring test.^{17,18} A fracture strength of 12 MPa was found for the SiC derived pine. For the high porous ceramic material, the low strength value was influenced by the pore fraction (71% in this case) and pore shape. Following Gibson and Ashby,¹⁹ the relative strength for plastic collapse of wood structure can be related with the relative density (ρ^*/ρ_s —relative density, ρ^* —the density of cell structure and ρ_s —the density of the fully dense material) as follows:

$$\frac{\sigma^*}{\sigma_s} = C_2 \left(\frac{\rho^*}{\rho_s} \right)^n$$

where, σ^* is the strength of the cellular structure, σ_s —the strength of the fully dense material, C_2 —the experimental constant and n , the exponential constant, is equal 1 in axial and 2 in tangential and radial direction.

Crack deflection during fracture results in a non-catastrophical fracture behavior. The stress-strain curve was nearly linear [Fig. 6(b)]. The cell walls were pulled apart at the middle lamella and cell wall peeling occurred [19] [Fig. 7(a,b)]. It can be seen that the crack propagate not continuously, but bridged along its path [Fig. 7(b)].

The capability of applying versatile shaping techniques makes wood an interesting precursor material for manufacturing of cellular ceramics. Si-vapor infiltration into pine-wood yields a single phase β -SiC with a porosity of 71% and a pore diameter of about 20 μm . Depending on the infiltration and reaction parameters the microscopical morphology, the grain size and specific surface area can be designed. Biomorphic SiC-ceramics with a

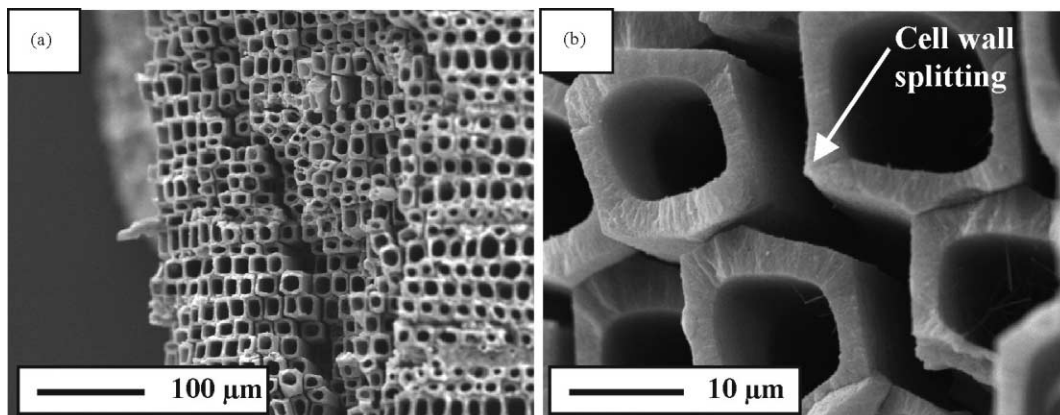


Fig. 7. Crack deflection induced during ball-on-ring test at SiC-derived from pine.

directed pore structure are promising materials for applications as high temperature filters or catalyst support structures.

Acknowledgements

The financial support from the Volkswagen Foundation under contract no. I/73 043 is gratefully acknowledged.

References

1. Gurfinkel, G., *Wood Engineering*, 2nd edn. Kendall/Hunt, Dubuque, Iowa, 1981.
2. D'Arcy N. Thompson, *On Growth and Form*, 2nd edn. Cambridge University Press, Cambridge, 1952.
3. Sieber, H., Hoffmann, C., Kaindl, A. and Greil, P., Biomimetic cellular ceramics. *Advanced Engineering Materials*, 2000, **2**(3), 105–109.
4. Patel, M. and Padhi, B. K., Production of alumina fibre through jute fibre substrate. *J. Mater. Sci.*, 1990, **25**, 1335–1343.
5. Patel, M. and Padhi, B. K., Titania fibres through jute fibre substrates. *J. Mater. Sci. Lett.*, 1993, **12**, 1234–1235.
6. Ota, T., Imaeda, M., Takase, H., Kobayashi, M., Kinoshita, N., Hirashita, T., Miyazaki, H. and Hikichi, Y., Porous titania ceramic prepared by mimicking silicified wood. *J. Am. Ceram. Soc.*, 2000, **83**(6), 1521–1523.
7. Sieber, H., Rambo, C., Cao, J., Vogli, E. and Greil, P., Manufacturing of porous oxide ceramics by replication of plant morphologies. *Key Eng. Mater.*, 2001, **206–213**, 2009–2012.
8. Vogt, U., Herzog, A., Graule, T., Klingner, R. and Zimmermann, T., Porous ceramics derived from wood. *Key Eng. Mater.*, 2001, **206–213**, 1941–1944.
9. Zollfrank, C., Kladny, R., Sieber, H., Greil, P. and Motz, G., Manufacturing of anisotropic ceramics from preceramic polymer infiltrated wood. *Ceram. Tran.* 128, *Advances in Ceramic Matrix Composites*, VII, ed. N. P. Bansal, J. P. Singh, H.-T. Lin, 2001.
10. Ota, T., Takahashi, M., Hibi, T., Ozawa, M., Suzuki, S., Hikichi, Y. and Suzuki, H., Biomimetic process for producing SiC “Wood”. *J. Am. Ceram. Soc.*, 1995, **78**, 3409–3411.
11. Vogli, E., Mukerji, J., Hoffman, Ch., Kladny, R., Sieber, H. and Greil, P., Conversion of oak to cellular silicon carbide ceramic by gas-phase reaction with silicon monoxide. *J. Am. Ceram. Soc.*, 2001, **84**(6), 1236–1240.
12. Sieber, H., Vogli, E., Müller, F., Greil, P., Popovska, N. and Gerhard, H., CVI-R gas phase processing of porous, biomimetic SiC-ceramics. *Key Eng. Mater.*, 2001, **206–213**, 2013–2016.
13. Greil, P., Lifka, T. and Kaindl, A., Biomimetic silicon carbide ceramics from wood I and II. *J. Eur. Ceram. Soc.*, 1998, **18**(14), 1961–1983.
14. Shin, D. W. and Park, S. S., Silicon/Silicon carbide composites fabricated by infiltration of a silicon melt into charcoal. *J. Am. Ceram. Soc.*, 1999, **82**, 3251–3253.
15. Martinez-Fernandez, J., Singh, M. and Valera-Feria, F. M., High temperature compressive mechanical behavior of biomimetic silicon carbide ceramics. *Scri. Mater.*, 2000, **43**, 813–818.
16. Byrne, C. E. and Nagle, D. C., Carbonization of wood for advanced materials applications. *Carbon*, 1997, **35**(2), 259–266.
17. Shetty, D. K., Rosenfield, A. R., McGuire, P., Bansal, G. K. and Duckworth, W. H., Biaxial flexure tests for ceramics. *Amer. Ceram. Soc. Bull.*, 1980, **59**(12), 1193–1197.
18. Ritter, J. E., Jakus Jr., K., Batakis, A. and Bandyopadhyay, N., Appraisal of biaxial strength testing. *J. Non Cryst. Sol.*, 1980, **38&39**, 419–424.
19. Gibson, L. J. and Ashby, M. F., *Cellular Solids: Structure and Properties*. Pergamon Press, New York, 1988.